Passive Flow Control over NACA0012 Aerofoil using Vortex Generators

V. T. Gopinathan[1],
Assistant Professor,
Department of Aeronautical Engineering,
Hindusthan College of Engineering and Technology,
Coimbatore, India.

M. Ganesh[2],
Assistant Professor,
Department of Aeronautical Engineering,
Hindusthan College of Engineering and Technology,
Coimbatore, India.

***Abstract*— Numerical simulations of turbulent flow over a NACA0012 aerofoil attached with vortex generators (VG) are carried out over a wide range of angles of attack at $Re=5.5\times10^5$ The three-dimensional Reynolds averaged Navier-Stokes equations along with closure equations of Spalart-Allmaras turbulence model are solved using commercial package FLUENT. The addition of VG results in increased lift-coefficient and reduced drag-coefficient at large incident angles. The influence of VG on the fluid flow and aerodynamic forces acting on the aerofoil are reported in this paper, with the emphasis on how the addition of the small vanes helps to delay the onset of stall. Comparison of streamline patterns, pressure coefficient and contour plots of field variables between the clean aerofoil and VG fitted aerofoil help us to understand how the vortex generator energises the boundary layer flow and hence delay the stall.**

Keywords — Vortex generator, flow control, delay of stall, streamwise vortex, tip vortex.

1. INTRODUCTION:

At low angles of attack (α), the flow over an airfoil is smooth and attached. When α is increased, the coefficient of lift (C_L) is increased as the pressure difference between the suction and pressure surface of the aerofoil is enhanced. However, after a particular α, known as stalling angle (α_s), the flow will not able to withstand the adverse pressure gradient generated over the suction side of the foil and as a result the boundary layer separation will take place (Anderson, 2001). This phenomenon is known as stalling which results in loss of lift, increased drag, generation of aerodynamic noise and onset of buffeting. An aircraft is required to operate at high α during takeoff, landing and maneuvering. Hence, flow control over an aerofoil at high angles of attack is of strong interest. Manypassive flow control devices are employed to mitigate the aforementioned adverse effects by delaying or suppressing the separation, and thereby widen the operating α range of aircraft wings (Gad-el-Hak, 1991).

Vortex generators (VGs) are an array of small vanes attached perpendicularly over the suction surface of the wings and in turbomachine blades. These vanes are fixed at a small incident angle (β) relative airflow. VGs enhance the ability of the fluid to stick with the wing surface even at large α by increasing the momentum transfer from the free-stream flow into the boundary layer.

The concept of VG is first introduced by Taylor, 1947. He has shown that the streamwise trailing vortices generated over a row of small plates increased the streamwise momentum and hence delay the flow separation in a diffuser. Subsequently many tests have been performed to show the effectiveness of VGs as a flow control device. The turbulent boundary layer developed over a flat plate at various adverse pressure gradients are studied by Schubauer and Spangenberg, 1960. Their study has shown that the introduction of VGs enhanced mixing in the boundary layer and hence the effective adverse pressure gradient is reduced.

The subsonic wind tunnel testing of a canard aerofoil from the Voyager aircraft showed that properly designed VGs were found to increase the lift and reduce the drag (Bragg and Gregorek, 1987). A wide variety of passive flow control devices were studied to understand their effectiveness in separation control (Lin et al, 1990, 1991, 1999). It has been concluded that VGs were more efficient in achieving the flow separation control by means of the streamwise vortices produced on them. The VGs producing counter-rotating streamwise vortices are much more efficient than that of producing co-rotating streamwise vortices.

Recently, Shan et al., 2008 performed flow control experiments over a NACA0012 aerofoil at $\alpha=6^0$ using passive and active VG configurations. The passive VGs reduce the recirculation length by almost 80%. However, since the active VGs generate streamwise vortices of strength exactly required to control the separation, they outperform passive VGs.

Experiments performed with VGs attached over the race car wings show that the addition of VGs increased the downward force (Kuya et al., 2009). Counter-rotating VGs not only increases the downward momentum transfer, they also produce less drag penalty. In some cases, it was observed that the performance of clean aerofoil was better than that of attached co-rotating VGs.

Majority of the studies focused on the effect of VGs have considered flow past a bump to mimic the adverse pressure gradient generated over the wings (Lin, 2002). Only few researchers considered the aerofoil configuration, and they reported the effectiveness of VG on the fluid flow only for a particular angle of attack (Shan et al., 2008). The objective of the present work is to analyze the influence of VGs on a NACA 0012 aerofoil for a wide range of angles of attack. The counter-rotating VG configuration is chosen, since it is more efficient than its co-rotating counterpart (Lin et al., 1991, Kuya et al., 2009).

2. GEOMETRY, GRID DETAILS AND NUMERICAL METHODOLOGY:

NACA 0012 aerofoil is used as the wing cross-section. The details of the dimensions of VG and its orientation are schematically shown in Fig. 1. All these details are taken from Shan et al.

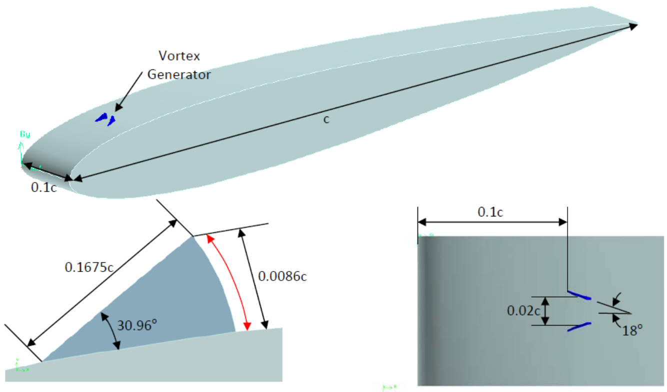

Figure 1. Illustration of the geometry and dimensions of the wing and vortex generator

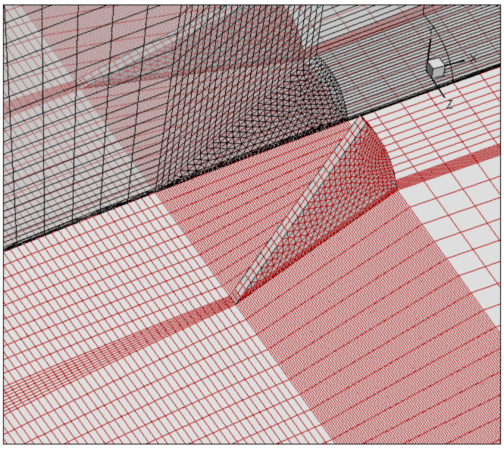

Figure 2. Zoomed view of mesh near the vortex generators

The three-dimensional steady incompressible Navier-Stokes equations are solved using commercial package FLUENT. The Reynolds number, Re (=Uc/ν, where U is the free-stream velocity, c is the chord length of the aerofoil and ν is the kinematic viscosity of the fluid) = 5.5×10^5. The second order implicit Euler backward scheme is used for temporal discretization.

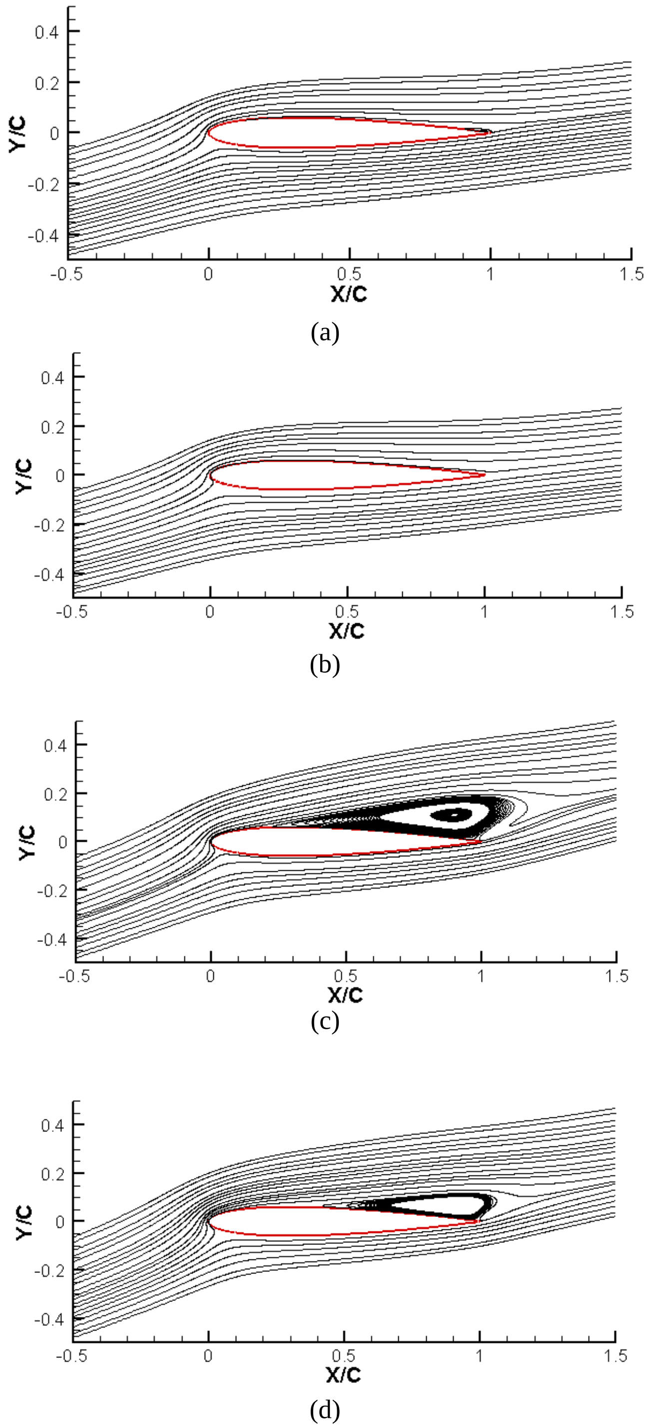

Figure 3. Streamline patterns over the mid-span plane of the aerofoil at, (a) $\alpha=11^0$ without VG (b) $\alpha=11^0$ with VG (c) $\alpha=16^0$ without VG (d) $\alpha=16^0$ with VG

The convective terms are approximated using second order upwind scheme. The Spalart-Allmaras model is used to model the influence of turbulent Reynolds stress terms in the momentum equations. The y+ value in our simulations are maintained below 3. In flows with adverse pressure gradient and separation, Spalart-Allmaras model provides more accurate results when compared to other models. Moreover, SA model is numerically very stable and is less sensitive to the grid resolution than two-equation models (Yaras and Grosvenor, 2003).

From the leading-edge of the aerofoil, the computational domain extends 5c upstream and 20c downstream. The top and bottom boundaries of the domain are located at 10c away from the foil. The whole computational domain is discretized with structured grid with dense mesh near the wing and VG, and coarse mesh away from them. The grid around the VG configuration is shown in Fig. 2. The number of points over the foil and VG are 300 and 100 respectively. The total number of mesh points in the whole domain is 1100395. These numbers are arrived at after carrying out a detailed grid-independency study.

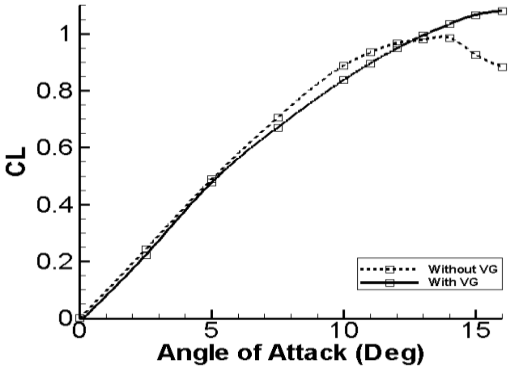

(a)

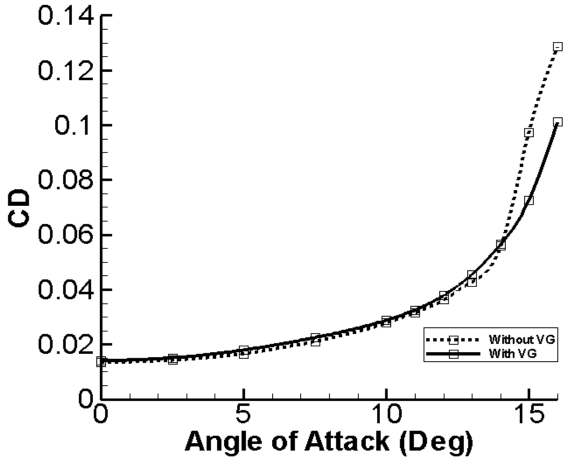

(b)

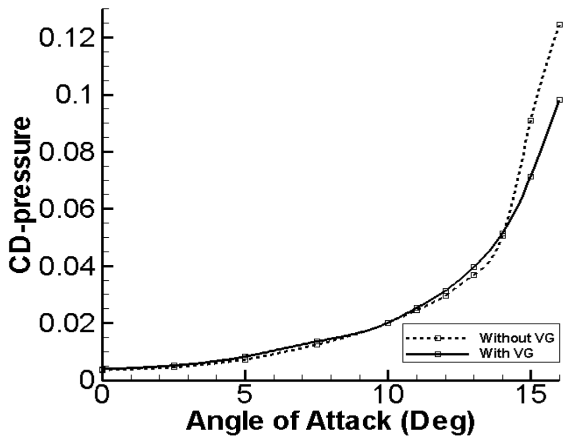

(c)

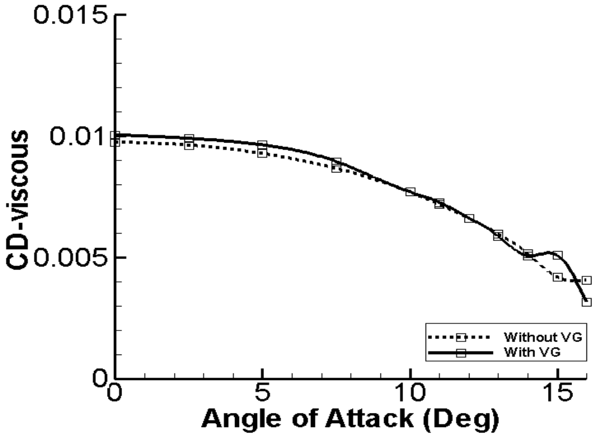

(d)

Figure 4. With respect to angle of attack, the variation of (a) Lift coefficient (b) Total Drag coefficient (c) Pressure drag coefficient (d) Skin-friction drag coefficient

The upstream boundary is modeled with a freestream velocity inlet, to match the Reynolds number of 5.5×10^5, based on the wing chord. An outflow boundary condition is imposed for the downstream boundary. The top, bottom and side boundaries are modeled with a symmetric condition. A no-slip boundary condition is applied on the wing surface and VGs.

3. RESULTS AND DISCUSSION:

To demonstrate the influence of VGs, first the viscous fluid flow over a clean aerofoil is simulated. Then, the VGs are fitted to the foil as in Fig. 1 and the simulations with same Re are carried out. The variations between these simulations show the influence of VG over the aerofoil. The numerical experiments are conducted in the angle of attack range from 0 to 16 degrees. Favorable effects of VGs are reported on aerodynamic force coefficients (C_L and C_D) and stalling angle. Moreover, how these modifications in force coefficients are achieved is explained in this section

3.1 Streamline patterns

Comparison of the streamline patterns shows qualitatively the influence of VG on the flow past the aerofoil. The streamline patterns on the mid-span plane for two different angles of attack are shown in Fig. 3. When $\alpha=11^0$, the streamlines of clean aerofoil and that of attached VG are almost the same and so are the aerodynamic force coefficients (Fig. 4). The flow is completely attached over the top surface of the foil. However, after the wing is stalled, the VGs help to reduce the length of the recirculation region (Fig. 3c and 3d). When there is no VG, the flow separates from the wing immediately after the leading edge and the large vortex can be seen in Fig. 3c. With the addition of VG, the size of the recirculation region is substantially reduced (Fig. 3d). The quantitative effect of this is discussed hereafter.

3.2 Effect of VG on Aerodynamic forces

The variation of lift (C_L) and drag coefficient (C_D) with respect to the angle of attack (α) are shown in Fig. 4. At low α, the difference between the clean aerofoil and that fitted with VG is not significant. However, for a clean aerofoil, the C_L decreases rapidly and C_D shows a sharp increase at $\alpha=14^0$ (Fig. 3a and 3b). From this, it can be inferred that the clean aerofoil is stalled at this α. In contrary to this, the aerofoil with VGs does not show any sign of stalling until $\alpha=16^0$, since throughout the range of α considered, the C_L as well as C_D increases gradually as can be seen from the figure. This result demonstrates the stall-delaying effect of vortex generators at high angle of attack flow over the aerofoil. The C_D of attached VG aerofoil is higher than that of clean aerofoil at low α (Fig. 4b), because at such low α, the skin-friction drag produced over the foil dominates the pressure drag due to the streamlined shape of the foil. Since the addition of VGs increases the wetting surface area available for the flow, the increase in C_D is observed (Fig. 4d). Moreover, the tip vortex produced from the VG also adds up to additional drag. But it can be seen from Fig. 3b that the increase in C_D produced by the VG is almost negligible. As α is increased, the contribution of pressure drag to the total drag is increased since the separation takes place at large α. The separation is delayed in aerofoil with attached VG. Hence C_D of attached VG case is lower than that of clean aerofoil. The reason for the increase of skin-friction in with VG case near $\alpha=14^0$ is not clear.

3.3 Effect of VG on Cp distribution

Figure 5 shows the distribution of pressure coefficient (Cp) over the aerofoil at two different angles of attack. The simulations of Shan et al., 2008 has shown that at $Re=10^5$ and $\alpha=6^0$ the addition of VGs has only minor influence in the Cp distribution. Except near the VG locations, the Cp of with and without VG coincide. In our simulations also, the influence of VG is almost negligible until $\alpha=11^0$ as shown in Fig. 5a. This is despite the difference in Re of Shan et al., 2008 and our simulations. In the clean aerofoil, the Cp achieves a minimum value near the leading-edge, owing to acceleration of the fluid flow over the top surface of the foil. Just after the peak value, the Cp increases along the downstream creating a strong adverse pressure gradient. This causes the boundary layer to separate from the top surface. Though, with the addition of VGs, the maximum suction peak remains the same, the subsequent rate of increase of Cp is less when compared to that of clean aerofoil case.

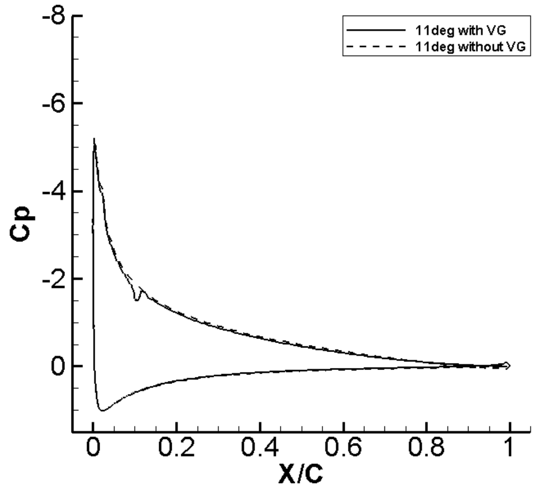

(a)

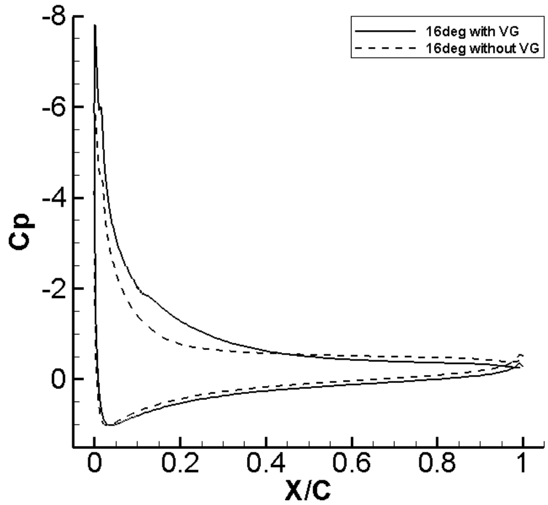

(b)

Figure 5.Cp distribution over the aerofoil with and without VG at (a) $\alpha=11^0$ (b) $\alpha=16^0$

This is advantageous in two ways. Firstly, the adverse pressure gradient over the aerofoil is decreased and hence the stalling is avoided. The reduction in adverse pressure gradient with the help of VGs has been reported by Schubauer and Spangenberg, 1960, and it is attributed to the effective mixing in the boundary layer. Secondly, the suction pressure prevails over most of the top surface of the foil. This is reflected in Fig. 4 as the increase in C_L at the same operating α.

3.4 Flow field induced by VG

Since the VGs are fitted to the aerofoil at a small incidental angle, the pressure difference between the both surfaces of the foil creates a tip vortex. The pathline plot of flow over the VG is given in Fig. 6. This is very similar to the creation of tip vortex in finite aspect ratio wings (Anderson, 2001). This tip vortex transports the high-momentum fluid from the outer layers into the boundary layer region.

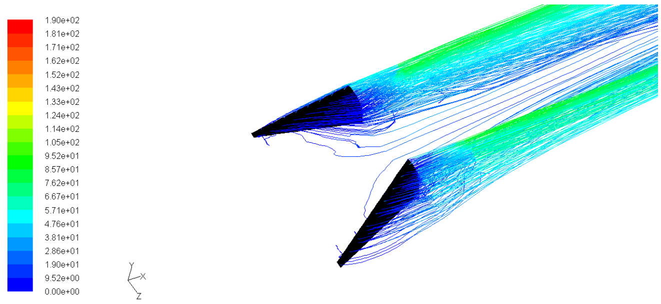

Figure 6.Pathlines over the vortex generators (colored with streamwise velocity)

Hence the effective momentum interaction between the outer layers and the boundary layer is enhanced. As a result, the retarded fluid flowing in the boundary layer region is energized to resist the adverse pressure gradient generated. In Fig. 6 the lines are colored with magnitude of streamwise vorticity. It can be seen that the streamwise velocity gets increased (see the color map) with the addition of VGs.

It has been stated that the adverse pressure gradient over the top surface of the foil is reduced with the addition of VGs at large α. The physical basis of this effect is explained here. The streamwise vortex generated as the tip vortex from VG induces a swirling flow in y-z plane. At the mid-plane between the VGs, the flow has a strong vertical component towards the wall of the aerofoil. The enhanced momentum transfer explained above is actually achieved by this induced vertical velocity. The vertical velocity directed towards the wall carries the high momentum fluid into the boundary layer and hence the kinetic energy of the near-wall fluid layers is increased. The vertical velocity moving away from the wall transports the low velocity fluid from the boundary layer to the outer flow region.

As has been pointed out by Godard and Stanislas, 2006, the VGs essentially modify the coherent structures of the boundary layer. Since RANS equations are solved here, the detailed study of near wall effects is not possible. To gain in depth knowledge on how VGs modify coherent structures and keep the flow attached over the aerofoil, direct numerical simulations (DNS) over this configuration are mandatory.

CONCLUSION

Flow separation control over a NACA0012 aerofoil using vortex generators is studied by performing numerical simulations. The influence of VGs on bulk quantities of the flow (C_L and C_D) is reported and the flow field modifications are discussed. The streamwise vortices produced from the VGs are of sufficient strength to delay the stalling for the angle of attack range considered in this study. Direct Numerical Simulations (DNS) over this configuration can shed more light on the fundamental physical understanding of the modifications in the coherent structures induced by the VGs to keep the boundary layer attached to the wall.

REFERENCES

[1] Anderson, J.D., 2001. Fundamentals of Aerodynamics, Third ed, McGraw-Hill publications.

[2] Bragg, M.B., Gregorek, G.M., 1987. Experimental study of airfoil performance with vortex generators, Journal of Aircraft 24, 305—309.

[3] Gad-el-Hak, M, Brushnell, D.M., 1991. Separation control: review, Journal of Fluids Engineering 113, 5—30.

[4] Godard, G, Stanislas, M, 2006. Control of a decelerating boundary layer. Part I: Optimization of passive vortex generators, Progress in Aerospace Sciences 10, 181—191.

[5] Kuya, Y, Takeda, K, Zhang, X, Beeton, S, Pandaleon, T, 2009. Flow separation control on a racecar wing with vortex generators, Journal of Fluids Engineering 131, 121102.

[6] Kuya, Y, Takeda, K, Zhang, X, Beeton, S, Pandaleon, T, 2009. Flow physics of racecar wing with vortex generators in ground effect, Jounral of Fluids Engineering 131, 121103.

[7] Lin, J.C., Howard, F.G., Brushnell, 1990. D.M., Investigation of several passive and active methods for turbulent flow separation control, AIAA paper 90—1598.

[8] Lin, J.C., Selby, G.V., Howard, F.G., 1991. Exploratory study of vortex-generating devices for turbulent flow separation control, AIAA paper 91—0042.

[9] Lin, J.C., 1999. Control of turbulent boundary layer separation using micro-vortex generators, AIAA paper 99—3404.

[10] Lin, J.C., 2002. Review of research in low-profile vortex generators to control boundary-layer separation, Progress in Aerospace Sciences 38, 389—420.

[11] Robinson, S.K., 1991. Coherent motion in the turbulent boundary layer, Annual Review of Fluid Mechanics 23, 601—639.

[12] Schubauer, G.B., Spangenberg, W.G., 1960. Forced mixing in boundary layers, Journal of Fluid Mechanics 8, 10—32.

[13] Shan, H, Jiang, L, Liu, C, Love, M, Maines, B, 2008. Numerical study of passive and active flow control over a NACA0012 airfoil, Computers and Fluids 37, 975—992.

[14] Taylor, H.D., 1947. The elimination of diffuser separation by vortex generators, United aircraft corporation Report No. R-4012-3.

[15] Yaras, M.I., Grosvenor, A.D., 2003. Evaluation of one- and two-equation low-Re turbulence models. Part I - Axisymmetric separating and swirling flows,International Journal for Numerical Methods in Fluids 42, 1293—1319.

[16] Yaras, M.I., Grosvenor, A.D., 2003. Evaluation of one- and two-equation low-*Re* turbulence models. Part II - Vortex-generator jet and diffusing S-duct flows, International Journal for Numerical Methods in Fluids 42, 1321—1343.